Received Date : 21-Apr-2016

Revised Date : 08-Aug-2016

Accepted Date : 10-Aug-2016

Article type : Research Article

In vitro study on potential pharmacological activity of Curcumin analogues and their copper complexes.

Erika Ferrari,*,† Rois Benassi,† Monica Saladini,† Giulia Orteca,† Zuzana Gazova,§ Katarina Siposova§

†*Department of Chemical and Geological Sciences, University of Modena and Reggio Emilia, 41125 Modena, Italy*

§*Department of Biophysics, Institute of Experimental Physics Slovak Academy of Sciences, Watsonova 47, 040 01 Kosice, Slovakia.*

***** corresponding author: email: erika.ferrari@unimore.it; tel. +39 059 2058631

ABSTRACT

Curcumin and its derivatives have attracted great interest in the prevention and treatment of Alzheimer's disease (AD), thanks both to the ability to hinder the formation of amyloid-beta (Aβ) aggregates and the ability to bind Cu (II) ion. In this article, we explore the ability of curcumin derivatives of K2T series to affect amyloid $A\beta_{1\text{-}40}$ aggregation. These derivatives were obtained by introducing the *t*-butyl ester group through a methylenic spacer on the central carbon atom of the β-diketo moiety of curcumin frame. The studied curcuminoids were demonstrated to inhibit $A\beta_{1\text{-}40}$ fibrillization at substoichiometric concentrations with IC_{50} value near that of curcumin.

This article has been accepted for publication and undergone full peer review but has not been through the copyediting, typesetting, pagination and proofreading process, which may lead to differences between this version and the Version of Record. Please cite this article as doi: 10.1111/cbdd.12847

In addition the antioxidant properties and DNA interaction of their Cu(II) complexes is evaluated. The structure of Cu(II)-K2T31 complex is also proposed on the basis of DFT calculation.

Keywords: curcumin analogues; Alzheimer's Disease; copper complexes; Aβ amyloid, protein aggregation inhibition.

1. INTRODUCTION

The growing interest of researchers towards curcumin and its derivatives is reflected by the large number of articles that are published every year on the subject by many different scientific journals. It is well known that curcumin possesses numerous interesting biological activities such as antioxidant, antiinflammatory, antimalarial and anticarcinogenic (1). Studies on the potential role of curcumin in the treatment of Alzheimer's disease (AD) have also been recently reported (2). The main cause of AD pathogenesis is attributed to a toxic peptide called amyloid-beta (Aβ), which is generated by the metabolism of the amyloid precursor protein and cleaved by the both β and γ-secretase within the brain (3). Aβ has a high aggregation ability and consequently its aggregate is very toxic (4-6). Therefore, it is widely believed that a drug that is able to inhibit Aβ fibrillization or dissociate the Aβ aggregate may become a promising treatment for AD. Since Aβ-induced oxidative stress in neuronal cells may be a cause of AD pathology, another pharmacological approach for AD is the development of antioxidant compounds for therapy. Therefore the natural antioxidant curcumin has been investigated as a potential compound for both prevention and treatment of AD (7, 8), and its Aβ disaggregation ability was demonstrated *in vitro* (9, 10). However, the use of curcumin *in vivo* is still limited by its poor bioavailability, which is in particular due to

its great instability under physiological condition (i.e. fast degradation in slightly basic environment) (11).

Another interesting feature of curcumin is its ability to strongly chelate metal ions through the keto-enolic moiety (12). Several authors reported that the interaction of curcumin with copper ion plays an important role in its pharmacological activity against different pathologies (13). In particular, some diseases are related to the presence of copper at high concentration, which generates oxidative radicals through the Fenton reaction. Elevated concentration of copper is observed in tumors and cancer tissues (14, 15). In addition copper induces Aβ aggregation (16), therefore the use of a chelating agent limits the free copper concentration and leads to improvement in disease conditions (17-19). Thus, chelation of copper by curcumin has been proposed as one of the possible mechanisms which potentially contributes to amyloid reduction, both *in vitro* (20) and in animal models (21).

Recently, our interest has been directed to the synthesis of curcumin derivatives showing greater chemical stability while maintaining almost unchanged the biological properties of the lead compound as a prelude to a good pharmacological activity. A wide variety of curcumin analogues were synthesized with structural modifications on both the aromatic rings and the di-ketonic group by the insertion of an alkyl substituent to the central carbon atom (22, 23). Among these derivatives, those with a *t*-butyl ester on central carbon atom, namely K2T series, showed higher chemical stability under physiological condition with respect to curcumin and showed cytotoxicity against different tumorigenic cell lines, with IC_{50} values similar to or in many cases lower than curcumin itself (23). The metal chelating ability of these curcumin analogues was also explored and they demonstrated good metal chelating properties both towards gallium(III) and copper(II) ions (24, 25).

In order to clarify the structure–activity relationship and the role of metal chelation in the biological properties of these compounds, we report a study on the ability of the compounds reported in **Scheme 1** to affect amyloid $A\beta_{1-40}$ aggregation. Furthermore, apart from favoring Aβ aggregation and radical processes (Fenton and Haber-Weiss reactions), the presence of loosely bound copper may also alter the biological properties of the ligands. In the case of curcumin, the reaction rate in scavenging DPPH radicals is 10 folds less for metal complex than free curcumin (13). For these reasons, we aimed to investigate the effect of metal ion coordination on antioxidant activity. Finally, Cu(II)-K2T potential interaction with DNA is investigated in order to derive relevant information on potential cytotoxicity of metal complexes.

2. MATERIALS AND METHODS

2.1 Chemistry

Elemental analysis was performed on a CE Instruments EA 1110. NMR spectra were recorded on a Bruker Avance AMX-400 spectrometer with a Broad Band 5 mm probe in inverse detection. Nominal frequencies were 100.13 MHz for ^{13}C, and 400.13 MHz for ^{1}H. Typical parameters were used for 2D COSY, HSQC, and HMBC experiments.

LC-MS spectra were recorded on 6310A ion trap LC-MS (Agilent Technologies) in isocratic condition (20% H_2O (0.1% HCOOH), 80% ACN) and in positive mode detection.

All chemicals were analytical reagent grade and used without further purification unless otherwise specified. They were purchased form Sigma-Aldrich. $A\beta_{1-40}$ was purchased from rPeptide (Cat # A-1001-2, Lot # 10290940T). The purity of all final compounds was determined to be at least 95% pure by a combination of HPLC, LCMS, NMR, and combustion analysis.

All the curcuminoids were synthesized and characterized as previously reported (23).

The Cu(II) complexes were obtained *in situ* by direct reaction of $CuCl_2$ water solution with curcuminoid methanolic solution to give 1:1 and 1:2 metal-to-ligand molar ratios, corresponding to the complex species CuL^+ and CuL_2 ($[Cu^{2+}]$=1.2mM).

2.2 Computational Details

All calculations were performed with the Gaussian 03 package of programs (26) and GaussView 03 (27) was used as the plotting tool for data visualization. The computations were performed by DFT approach, and the structures were fully optimized using hybrid-functional B3LYP with 6-311G** basis set (B3LYP/6-311G**). The selection of DFT basis set was made considering the dimension of molecules and taking into account our previous experience on these systems (28).

2.3 Amyloid fibrillization of Aß$_{1-40}$ peptide

$A\beta_{1-40}$ was dissolved in 10 mM NaOH to stock concentration of 665 μM, sonicated for 1 min in a bath sonicator, and centrifuged for 10 min (12 000 g) at 4°C to precipitate large aggregates. The $Aß_{1-40}$ stock solution was then diluted to final concentration of 10 μM in 150 mM 3-(N-morpholino)-propanesulfonic acid (MOPS) with 0.035% of NaN_3, pH 6.9 and incubated for 7 days at 37°C. The formation of amyloid fibrils was monitored by characteristic changes in Thioflavin T fluorescence (ThT assay), and visualized by atomic force microscopy.

2.4 Thioflavin (ThT) assay

Thioflavin T was added to the samples containing 10 μM of $A\beta_{1-40}$ to a final concentration of 20 μM (after finishing amyloid fibrillization, i.e. after 7 days incubation at 37°C). After 1 hour incubation at 37°C, the fluorescence intensities measurements were performed in a 96-well plate by a Synergy MX (BioTek) spectrofluorimeter. The excitation was set at 440 nm and the emission recorded at 485 nm. The excitation and

emission slits were adjusted to 9.0/9.0 nm and the top probe vertical offset was 6 mm. All ThT fluorescence experiments were performed in triplicate and the final value is the mean of measured values.

2.5 Atomic Force Microscopy - AFM

Samples for AFM were prepared by spreading solutions on a freshly cleaved mica surface and leaving them for 5 min to adsorb on the surface. After 5 min adsorption, the samples were washed with ultrapure water (18.2 MΩ cm) and left to dry. The protein concentration of 10 μM and studied compounds of 100 μM were used. AFM images were taken using a Scanning Probe Microscope (Veeco di Innova, Bruker AXS Inc., Madison, USA) in a tapping mode using an NCHV cantilever with specific resistance of 0.01 – 0.025 Ω cm, antimony (n) doped Si, radius of the tip curvature of 10nm. The resolution of image was 512 pixels per line (512 x 512 pixels/image) and scan rate 0.25-0.5 kHz.

2.6 Quantification of the inhibiting activity (IC_{50} values) of the curcuminoids.

Quantification of the curcuminoid inhibiting activity (IC_{50} values) was examined by measuring the ability of the compounds to inhibit the formation of amyloid aggregates for compound concentrations between 10 pM and 0.5 mM at fixed 10 μM peptide concentration. Curcuminoid was added to 10 μM native $A\beta_{1-40}$ solution and then the fibrillization was achieved by incubation at 37°C for 7 days. The amount of amyloid aggregates was observed by the ThT assay. The fluorescence intensities of the samples containing compound were normalized to the fluorescence signal of amyloid aggregates alone. The IC_{50} values were determined from dose-response curves obtained by fitting the average values by non-linear least-square method (SigmaPlot: sigmoidal, 3-parameters logistic: $y = a/1+(x/x_0)^b$). To measure the intrinsic fluorescence of the tested compounds the peptide was replaced with buffer solution. The volume of DMSO in

measuring samples was lower than 2% and has no effect on the stability of fibrils and $A\beta_{1\text{-}40}$ peptide fibrillization.

2.7 Antioxidant Activity (DPPH Radical Scavenging Method)

The antioxidant activity of the compounds was determined in terms of hydrogen donating or radical scavenging ability, using the stable radical DPPH. A variable amount (15, 30, 45, 75, 105 and 150 μL) of a methanol solution (1.2 mM) of each compound (curcuminoid (L), Cu(II) complexes (CuL_2)), including curcumin as benchmark, was placed in a cuvette, and 3 mL of a 6×10^{-5} M methanol solution of DPPH was added. Absorbance measurements were initiated immediately. The decrease in absorbance at 517 nm was determined continuously every minute up to 5', then every 5' up to 30' and every 30' until reaction reaches completion and absorbance stabilizes attaining a plateau after 120'. Methanol was used to zero the spectrophotometer. The absorbance of the DPPH radical without antioxidant, *i.e.* the control, was measured daily, and concentration was calculated applying **Equation 1** (29)**:**

$$\textbf{Eq. 1.} \qquad \left[\text{DPPH}^{\bullet}\right] = \frac{A - 1.006}{10970}$$

The percentage of inhibition (%In) of the DPPH radical by each sample was calculated according to the formula:

$$\%\text{In} = \frac{A_0 - A_t}{A_0} \times 100$$

where A_0 represents the absorbance of the control (DPPH radical) at time 0, while A_t refers to the absorbance of the mixture DPPH/antioxidant at time t (120 min). Values of absorbance were corrected taking into account volume dilution and all determinations were performed in triplicate.

2.8 Spectroscopic study on DNA interaction

All the experiments involving the interaction of the complexes with *calf thymus* DNA (*ct*-DNA) were carried out in Tris-HCl buffer (5 mM, pH 7.2). A solution of *ct*-DNA in the buffer gave a ratio of UV absorbance at 260 and 280 nm of about 1.8–1.9:1, indicating that the DNA was sufficiently free from protein (30). The DNA concentration per nucleotide and polynucleotide concentration were determined by absorption spectroscopy using the molar extinction coefficient (6600 $M^{-1}cm^{-1}$) at 260 nm (31). The intrinsic binding constant K_b for the interaction of these metal(II) complexes (CuL^+ and CuL_2) with DNA has been calculated from the absorption spectral titration data. The intrinsic binding constant K_b was determined from **Equation 2** (32):

Eq. 2 $[DNA]/(\varepsilon_A-\varepsilon_f) = [DNA]/(\varepsilon_B-\varepsilon_f) + 1/K_b(\varepsilon_B-\varepsilon_f)$

where [DNA] is the concentration of DNA in base pairs, the apparent absorption coefficient ε_A, ε_f and ε_B correspond to $A_{obs}/[M]$, the extinction coefficient of the free compound and the extinction coefficient of the compound when fully bound to DNA, respectively. Plot of $[DNA]/(\varepsilon_A-\varepsilon_f)$ vs. [DNA] gave a straight line with a slope of $1/(\varepsilon_B-\varepsilon_f)$ and an intercept of $1/K_b(\varepsilon_B-\varepsilon_f)$ and K_b was determined from the ratio of the slope to intercept.

3 RESULTS AND DISCUSSION

3.1 Effect on the Aß$_{1-40}$ amyloid fibrillization.

Thioflavin T (ThT) assay is regularly used for the investigation of the poly-peptide amyloid fibrillization because fluorescence intensity of ThT in presence of amyloid fibrils is significantly higher compared to proteins in native state, molten globule, unfolded state, or amorphous aggregates. The same applies in the case of $A\beta_{1-40}$ peptide.

Figure 1A reports the fluorescence intensities determined for soluble $A\beta_{1-40}$ peptide (black dotted line) and after the process of fibrillization for $A\beta_{1-40}$ alone (violet solid line). In addition, it is important to know if curcumin derivatives alone or in presence of ThT have emission fluorescence spectra in the studied range (465–600 nm) at excitation wavelength 440 nm. Presence of fluorescence signal in these wavelengths makes it impossible to investigate interference of compound with amyloid aggregation using ThT assay. For this reason compound K2T24, which has high fluorescence intensity, was excluded from the current study. The other curcumin derivatives had no significant fluorescence signal even at high concentrations as it is shown for K2T21 derivative in **Figure 1A** (red dash-dotted-dotted).

The interference of the curcuminoid with $A\beta_{1-40}$ amyloid fibrillization was first examined at two compound concentrations, namely for 100 μM and 100 nM (at 10 μM peptide concentration). After the process of $A\beta_{1-40}$ amyloid fibrillization (see Experimental Section) the fluorescence intensities were measured for $A\beta_{1-40}$ peptide and $A\beta_{1-40}$ peptide treated with curcuminoids using ThT fluorescence assay.

In **Figure 1A** the fluorescence spectra are shown for K2T21 derivative. The ThT intensities were normalized to the fluorescence detected for untreated sample of $A\beta_{1-40}$ after the process of fibrillization and are shown in **Figure 1B**: the lower the value of fluorescence intensity the more effective the fibrillization inhibition by the tested curcuminoids. At lower concentration (100 nM), a decline of ThT fluorescence was observed, and all the three derivatives (K2T21, K2T23 and K2T31) showed some inhibition with respect to the untreated sample.

At higher concentration (100 μM), a more significant fibrillization inhibition was observed, for all the compounds, despite a levelling in their activity. Fluorescence was

quenched greater than 80% in comparison to the control (untreated sample) for all curcuminoids.

To obtain more precise data, the inhibiting abilities of K2T derivatives were studied at varying the compound concentration in the range 10 pM - 1mM at fixed $A\beta_{1-40}$ concentration (10μM) using ThT assay. The observed relative fluorescence intensities (normalized to the fluorescence signal of $A\beta_{1-40}$ amyloid aggregates without curcuminoid) are shown in **Figure 2**.

The investigated curcuminods inhibit formation of fibrils in a concentration-dependent manner, and the decrease of fluorescence intensities follows a sigmoidal decay. From profiles, the concentrations at 50% decrease of the protein in the form of amyloid fibrils (IC_{50} values) were calculated. The obtained IC_{50} values equal to 12.5 ± 0.9 μM (K2T21), 8.1 ± 0.9 μM (K2T23), 7.5 ± 0.9 μM (K2T31) imply that these curcuminoids interfere with $A\beta_{1-40}$ peptide during fibrillization already at sub-stoichiometric concentrations.

The interaction of studied curcuminoids with $A\beta_{1-40}$ amyloid fibrillization was studied also using atomic force microscopy (AFM). AFM technique confirmed that 7 days incubation of soluble $A\beta_{1-40}$ peptide at pH 6.9, 37°C leads to the formation of characteristic fibrils with typical amyloid morphology (**Figure 3A**). The presence of curcuminoids causes changes in the morphology of Aβ fibrils, in fact the amount of the fibrillar aggregates significantly decreased and only short fibrillar or globular aggregates are observed (**Figure 3 B**, **C** and **D**). AFM images strongly support the data obtained by ThT assay.

According to IC_{50} values, the three curcuminoids inhibit $A\beta_{1-40}$ fibrillization with roughly equal affinities, and K2T23 and K2T31 seem to be the most active ones.

The literature data for the parent compound curcumin are still not consistent, in fact some authors report that curcumin inhibits the formation of Aβ fibrils from $A\beta_{40}$ and $A\beta_{42}$ and their extensions, as well as destabilizes preformed Aβ fibrils (IC_{50} = 0.19–0.63 μM (33); IC_{50} 0.679 μM (34)), while others report that curcumin inhibits Aβ oligomerization (IC_{50} 361.11±38.91 μM) but does not restrain fibrillization *in vitro* at concentrations between 30 and 300 μM (35). This discrepancy in IC_{50} values may be due to the extreme chemical instability of curcumin in simulated physiological conditions, from this point of view, K2T derivatives demonstrated a greater stability with respect to curcumin (23), therefore a better reproducibility of the results may be expected, in particular for K2T23 which is the most stable one among the investigated derivatives.

3.2 Free Radical Scavenging Ability

Free radical scavenging ability of Cu(II) complexes (CuL_2) is here evaluated by the DPPH radical assay, which is one of the most widely used method to determine antioxidant activity. Results, summarized in **Figure 4** and **Table 1**, point out that copper complexes can be divided into two main groups according to their DPPH inhibition, expressed by the percentage of inhibition and by EC_{50} (the antioxidant concentration necessary to decrease the initial amount of DPPH radical by 50%).

K2T21 and K2T31 Cu(II) complexes show a percentage of inhibition lower than curcumin complex, but they maintain a similar EC_{50} value in the range 25-35μM; while K2T23 and K2T24 exhibit very poor antioxidant ability confirming the fundamental role of the hydroxyl substituent on the aromatic ring as suggested by Priyadarsini *et al.* (36). Among the different reaction mechanisms proposed to explain antioxidant properties of curcumin, the involvement of keto-enolic group in stabilizing the formed radical through delocalization over the conjugated segments is also reported (37).

In K2T derivatives, the presence of a bulky substituent on central carbon atom of β-diketo moiety shifts the tautomeric equilibrium in favor of the diketo form in polar/protic medium, hence reducing the possible radical delocalization with a consequent diminishing of radical scavenging ability with respect to the leading compound curcumin (38).

Similarly, the presence of copper ion coordinated by the keto-enolic group prevents the involvement of keto-enolic moiety in the radical delocalization, so further increasing EC_{50} with regard to the free ligand. The lower antioxidant ability of K2T31 compared to K2T21 is not surprising, and it is reflected also in the respective Cu(II) complexes. The same observation was found comparing *bis*-demethoxycurcumin and curcumin suggesting the involvement also of methoxyl groups in antioxidant activity (39).

3.3 Theoretical DFT calculations

DFT calculations on K2T31 were performed in order to predict a possible structure of [Cu $(K2T31)_2$] complex and to elucidate the antioxidant properties of metal complexes, in particular the ability to scavenge DPPH. The theoretical calculation confirms that *in vacuo* the keto–enol tautomer is the most stable one as previously observed for curcumin and other substituted curcuminoids (22).

The more stable conformer of K2T31 was taken into account for further calculations, and, according to previous studies on Cu^{2+}-curcumin complex (40, 41), the M:L 1:2 chelating mode with a square planar arrangement was used as the starting point of our study to predict copper complexes. **Figure 5** reports the two different structural isomers of the complex, namely **A** and **B**, together with their energy values. The more stable conformer is **A,** although the difference in energy is very small (0.08 Kcal/mol). The O-H bond dissociation energy (BDE) was also calculated and **Table 2**

reports its value for the metal complex and free K2T31 in comparison with curcumin and parent K2T21. This theoretical parameter has been recognized appropriate for measuring the H atom donating ability related to antioxidant activity (39), the lower the BDE value, the higher the antioxidant activity. K2T31 shows a BDE value similar to that of K2T21 and curcumin, although the ability to scavenger DPPH radical is lower than that of K2T21 and curcumin itself. This finding confirms that, in addition to hydrogen homolytic dissociation, showed by BDE, the stabilization by resonance of the formed radical plays a fundamental role in radical scavenging properties. In fact, the prevalence in K2T31 of the DK form in solution together with the absence of the methoxyl substituent probably reduce the radical delocalization, so diminishing the activity against DPPH radical. In addition the BDE values of the metal complexes are greater than the free ligand, and agree well with the diminished DPPH scavenging ability previously observed for the Cu(II) complexes in comparison with the free ligands.

3.4 DNA binding

The binding of small molecules to DNA produces hypochromism, a broadening of the envelope, and a red shift of the complex absorption band. These effects are particularly pronounced for intercalators and the extent to which hypochromism occurs depends on the intercalative binding strength (42). In the case of groove binders, a wavelength shift may be observed, usually correlated with a conformational change on binding or complex formation (43). Curcumin binds to the major and minor grooves of DNA duplex as well as to the back bone phosphate groups, and no conformational changes were observed upon curcumin interaction with DNA (44)

The interaction with DNA is not the focus of this manuscript, however we think that collecting some data on K2T potential interaction with DNA is relevant in order to derive information on cytotoxicity, since they are able to penetrate into the cell nuclei.

The characteristic change in absorption spectra occurring during titration of Cu(II)-K2T21 (1:1) complex with *calf thymus* DNA (*ct*-DNA) is shown in **Figure 6**. The absorption spectra of the complex exhibited peaks in the range 350–450 nm having absorption maxima at 428 nm. The addition of *ct*-DNA to the complex solution results in a decrease in the absorption and a slight red shift (**Table 3**).

A similar behavior is observed also for the other Cu(II)-K2T complexes in 1:1 molar ratio, while no significant changes are shown in the UV-vis spectra by adding *ct*-DNA to M:L 1:2 complexes. The performance of 1:2 complexes may be attributed to the presence of two bulky ligands, which strongly prevent stacking interaction between aromatic chromophore and base pairs of DNA, hindering an intercalative binding to DNA. The steric hindrance of the ligand probably influences as well the value of binding constant, which is diminished with respect to curcumin (**Table 2**) and among the K2T series the bulkiest (K2T24) is the one which has the lowest value of K_b. In addition the involvement of Cu(II) ion in the coordination with DNA in 1:1 complexes cannot be excluded.

4. CONCLUSIONS

Due to its multi-faceted pharmacology, many studies have paved the way to the possibility of using curcumin for the treatment and/or prevention of neurodegenerative diseases, especially Alzheimer's disease (AD), with encouraging results. Nonetheless,

curcumin's low stability and bioavailability under physiological conditions has stimulated research to design new derivatives in order to overcome these drawbacks.

In the present study, curcumin K2T analogues were demonstrated to inhibit $A\beta_{1-40}$ fibrillization at substoichiometric concentrations with IC_{50} values near to that of curcumin.

Since metal ion homeostasis is tightly regulated to maintain physiological processes, imbalances of metal ions concentration, especially Cu^{2+}, may favor Aβ aggregation and subsequently induce oxidative damage. The use of copper(II) chelating agents, such as K2T compounds, may reduce the damage given by the free metal ion. The antiradical activity of copper(II) metal complexes in the M:K2T 1:1 and 1:2 molar ratio demonstrated that only K2T21, and in minor extent K2T31, hold the capacity to scavenge DPPH radical, suggesting the importance of a phenolic group combined with methoxyl moiety in *ortho* position.

In addition, Cu(II) complexes of K2T compounds, at 1:1 M:L molar ratio, interact with DNA, and in particular K2T21 and K2T31 showed binding constants of the same order of magnitude as curcumin, while the absence of the phenolic groups in K2T23 and K2T24 with a reduction in polarity in the first, and the presence of a bulky substituent (acetyl) in the latter dramatically decrease the values of DNA-binding constant.

Summarizing, among K2T series, K2T21 is the best candidate to develop new curcumin-based analogues able to combat AD for its multi-faced intrinsic characteristics: i) it is able to inhibit $A\beta_{1-40}$ aggregation, ii) it was demonstrated to tightly bind Cu(II) giving more stable complexes with respect to curcumin (ΔE = -3.59 Kcal/mol (23)), reducing metal concentration in the free form and consequently limiting $A\beta_{1-40}$ aggregation; iii) Cu(II):K2T21 1:1 complex maintains good radical scavenging

ability and DNA binding ability; iv) K2T21 is more stable than curcumin in physiological conditions, suggesting higher bioavailability.

ACKNOWLEDGEMENTS

This work was supported by Project VEGA 0181 and EU grant 26220220005.

Ferrari E. wants to thank the *Fondazione Cassa di Risparmio di Vignola* for supporting the project "Diagnosi precoce della malattia di Alzheimer: nuovi agenti diagnostici bi-modali per *imaging:* RAD (radiotracers for Alzheimer's Disease)".

REFERENCES

1. Esatbeyoglu T., Huebbe P., Ernst, I. M. A; Chin, D.; Wagner, A. E.; Rimbach, G. (2012) Curcumin-from molecule to biological function. Angew Rev; 51: 5309-5332.

2. Hishikawa N., Takahashi Y., Amakusa Y., Tanno Y., Tuji Y., Niwa H., Murakami N., Krishna U. K. (2012) Effects of turmeric on Alzheimer's disease with behavioral and psychological symptoms of dementia. Ayu; 33: 499–504.

3. Hashimoto M., Rockenstein E., Crews L. (2003) Role of protein aggregation in mitochondrial dysfunction and neurodegeneration in Alzheimer's and Parkinson's diseases. Neuro Mol Med; 4: 21-35.

4. Swerdlow R. H. (2007) Pathogenesis of Alzheimer's disease. Clin Interv Aging; 2: 347-359.

5. Minter M. R., Taylor J. M., Crack P. J. (2016) The contribution of neuroinflammation to amyloid toxicity in Alzheimer's disease. J Neurochem; 136: 457-474.

6. Pooler A. M., Polydoro M., Maury E. A., Nicholls S. B., Reddy S. M., Wegmann S., William C., Saqran L., Cagsal-Getkin O., Pitstick R., Beier D. R., Carlson G. A., Spires-Jones T.,

Hyman B. T. Amyloid accelerates tau propagation and toxicity in a model of early Alzheimer's disease. Acta Neuropath Comm; 3:14-24.

7. Lim G. P., Chu T., Yang F., Beech W., Frautschy S. A., Cole G. M. (2001) The Curry Spice Curcumin Reduces Oxidative Damage and Amyloid Pathology in an Alzheimer Transgenic Mouse. J Neurosci; 21: 8370-8377.

8. Varadarajan S., Yatin S., Aksenova M., Butterfield D. A. (2000) Alzheimer's amyloid beta-peptide-associated free radical oxidative stress and neurotoxicity. J Struct Biol; 130: 184–208.

9. Begum A. N., Jones M. R., Lim G. P., Morihara T., Kim P., Heath D. D., Rock C. L., Pruitt M. A., Yang F., Hudspeth B., Hu S., Faull K. F., Teter B., Cole G. M., Frautschy S. A. (2008) Curcumin Structure-Function, Bioavailability, and Efficacy in Models of Neuroinflammation and Alzheimer's Disease. J Pharmacol Exp Ther; 326: 196-208.

10. Hamaguchi T., Ono K., Murase A., Yamada M. (2009) Phenolic Compounds Prevent Alzheimer's Pathology through Different Effects on the Amyloid-β Aggregation Pathway. Am J Pathol; 175: 2557-2565.

11. Ringman J. M., Frautschy S. A., Cole G. M., Masterman D. L., Cummings J. L. (2005) A potential role of the curry spice curcumin in Alzheimer's disease. Curr Alzheimer Res; Apr. 131-136.

12. Heger M., van Golen R. F., Broekgaarden M., Michel M. C. (2014) The molecular basis for the pharmacokinetics and pharmacodynamics of curcumin and its metabolites in relation to cancer. Pharmacol Rev; 66: 222-307.

13. Barik A., Mishra B., Shen L., Mohana H., Kadamc R. M., Duttad S., Zhangb H. Y., Priyadarsini K. I. (2005) Evaluation of a new copper(II)-curcumin complex as superoxide dismutase mimic and its free radical reactions. Free Radical Bio Med; 39: 811-822.

14. Yoshida D., Ikeda Y., Nakazawa S. (1993) Quantitative analysis of copper, zinc and copper/zinc ratio in selected human brain tumor. J Neuro Oncol; 16: 109-115.

15. Gupte A., Mumper R. J. (2009) Elevated copper and oxidative stress in cancer cells as a target for cancer treatment. Cancer Treat Rev; 35: 32-46.

16. Atwood C. S., Moir R. D., Huang X., Scarpa R. C., Bacarra N. M., Romano D. M., Hartshorn M. A., Tanzi R. E., Bush A. (1998) Dramatic aggregation of Alzheimer a beta by Cu(II) is induced by conditions representing physiological acidosis. J Biol Chem; 273: 12817-12826.

17. Savelie M. G., Lee S., Liu Y., Lim M. H. (2013) Untangling Amyloid-β, Tau, and Metals in Alzheimer's Disease. ACS Chem Biol; 8: 856-865.

18. M. Tegoni, D. Valensin, L. Toso and M. Remelli (2014) Copper Chelators: Chemical Properties and Bio-medical Applications Curr Med Chem; 21:3785-3818.

19. Kochi A., Lee H. J., Vithanarachchi S. A., Padmini V., Allen M. J., Lim M. H. (2015) Inhibitory Activity of Curcumin Derivatives Towards Metal-Free and Metal-Induced Amyloid-β Aggregation. Curr Alzheimer Res; 12: 415-423.

20. Wanninger S.; Lorenz, V.; Subhan, A., Edelmann F. T. (2015) Metal complexes of curcumin – synthetic strategies, structures and medicinal applications. Chem Soc Rev; 44: 4986-5002.

21. Baum L., Ng A. (2004) Curcumin interaction with copper and iron suggests one possible mechanism of action in Alzheimer's disease animal model. J Alzheimer Dis; 6: 367-377.

22. Ferrari E., Saladini M., Pignedoli F., Spagnolo F., Benassi R. (2011) Solvent effect on keto-enol tautomerism in a new β-diketone: a comparison between experimental data and different theoretical approaches. New J Chem; 35: 2840–2847.

23. Ferrari E., Pignedoli F., Imbriano C., Marverti G., Basile V., Venturi E., Saladini M. (2011) Newly synthesized Curcumin based drugs: crosstalk between chemico-physical properties and biological activity. J Med Chem; 54: 8066-8077.

24. Ferrari E., Benassi R., Sacchi S., Pignedoli F., Asti M., Saladini M. (2014) Curcumin derivatives as metal-chelating agents with potential multifunctional activity for pharmaceutical applications. J Inorg Biochem; 139: 38-48.

25. Asti M., Ferrari E., Croci S., Atti G., Rubagotti S., Iori M., Capponi P. C., Zerbini A., Saladini M., Versari A. (2014) Synthesis and characterization of ^{68}Ga-labeled curcumin and curcuminoid complexes as potential radiotracers for Imaging of Cancer and Alzheimer' s Disease. Inorg Chem; 53: 4922-4933.

26. Gaussian 03, Revision D.01, Frisch M. J. et al. Gaussian, Inc., Wallingford CT (2004).

27. Dennington II R., Keyth T., Millam J., Eppinnett K., Hovell W. L., Gilliand R., Gaussview, Version 3.0, Semichem, Inc., Shawnee Mission, KS (2003).

28. Ferrari E., Asti M., Benassi R., Pignedoli F., Saladini M. (2013) Metal binding ability of curcumin derivatives: a theoretical *vs.* experimental approach. Dalton Trans; 42: 5304-5313.

29. Szabo M. R., Idiţoiu C., Chambre D., Lupea A. X. (2007) Improved DPPH Determination for Antioxidant Activity Spectrophotometric Assay. Chem Pap; 67: 214-216.

30. Satyanarayana S., Dabrowiak J. C., Chaires J. B. (1993) Tris (phenanthroline) ruthenium(II) enantiomer interactions with DNA: Mode and specificity of binding. Biochem; 32: 2573–2584.

31. Barton J. K., Goldberg J. M., Kumar C. V., Turro N. J. (1986) Binding modes and base specificity of tris(phenanthroline)ruthenium(II) enantiomers with nucleic acids: tuning the stereoselectivity. J Am Chem Soc; 108: 2081–2088.

32. Pyle A. M., Rehmann J. P., Meshoyrer R., Kumar C. V., Turro N. J., Barton J. K. (1989) Mixed-ligand complexes of ruthenium(II): factors governing binding to DNA. J Am Chem Soc; 111: 3053–3063.

33. Hamaguchi T., Ono K., Yamada M. (2010) Curcumin and Alzheimer's Disease. Neurosc & Therap; 16: 285–297.

34. Kim H., Park B. S., Lee K. G., Choi C. Y., Jang S. S., Kim Y. H., Lee S. E. (2005) Effects of naturally occurring compounds on fibril formation and oxidative stress of beta-amyloid. J Agric Food Chem; 53: 8537–8541.

35. Smith D. G., Cappai R., Barnham K. J. (2007) The redox chemistryof the Alzheimer's disease amyloid beta peptide. Biochim Biophys Acta; 1768: 1976–1990.

36. Priyadarsini K. I., Maity D. K., Naik G. H., Sudheer Kumar M., Unnikrishnan M. K., Satav J. G., Mohan H. (2003) Role of phenolic O-H and methylene hydrogen on the free radical reactions and antioxidant activity of curcumin. Free Rad Biol Med; 35: 475-484.

37. Galano A., Álvarez-Diduk R., Ramírez-Silva M. T., Alarcón-Ángeles G., Rojas-Hernández A. (2009) Role of reacting free radicals on the antioxidant mechanism of curcumin. Chem Phys; 363: 13-23.

38. Nardo L., Maspero A., Selva M., Bondani M., Palmisano G., Ferrari E., Saladini M. (2012) Excited-State dynamics of bis-dehydroxycurcumin carboxykic acid, a water-soluble derivative of the photosensitizer curcumin. J Phys Chem A; 116: 9321-9330.

39. Somparn P., Phisalaphong C., Nakornchai S., Unchern S., Morales N. P. (2007) Comparative antioxidant activities of curcumin and its demethoxy and hydrogenated derivatives. Biol Pharm Bull; 30: 74-78.

40. Shen L., Zhang H. Y., Ji H. F. (2005) A theoretical study on Cu(II)-chelating properties of curcumin and its implications for curcumin as a multipotent agent to combat Alzheimer's disease. J Mol Struct THEOCHEM; 757: 199–202.

41. Addicoat M. A., Metha G. F., Kee T. W. (2011) Density functional theory investigation of Cu(i)- and Cu(II)-curumin complexes. J Comput Chem; 32: 429–438.

42. Rajesh J., Rajasekaran M., Rajagopal G., Athapann P. (2012) Analytical methods to determine the comparative DNA binding studies of curcumin in Cu(II) complexes. Spectr Acta A; 97: 223-230.

43. Pruitt J. R., Pinto D. J., Estrella M. J., Bostrom L. L., Knabb R. M., Wong P. C, Wright M. R., Wexler R. R. (2000) Isoxazolines and Isoxazoles as Factor Xa Inhibitors. Bioorg Med Chem Lett; 10: 685-689.

44. Nafisi S., Adelzadeh M., Norouzi Z., Sarbolouki M. N. (2009) Curcumin Binding to DNA and RNA. DNA & Cell Biol; 28: 201-208.

Table 1. Percentage of inhibition referred to compound/DPPH at 1:1 molar ratio and EC_{50} value, [DPPH] = 6×10^{-5} M.

	% inhibition		EC_{50} (μM) esd ± 1 μM	
	Free ligand	Cu(II)-L	Free ligand	Cu(II)-L
Curcumin	96.05[23]	95.3	13[22]	19
K2T21	95.03[23]	77.5	16[22]	27
K2T31	87.8	65.7	23	36
K2T23	24.50[23]	24.5	/	/
K2T24	30.04[23]	21.6	/	/

Table 2. B3LYP/6-311G** calculated O-H (phenolic) bond dissociation energy BDE (kcal/mol).

	O-H BDE[a]
$Cu(K2T31)_2$ (cis)	109.25
$Cu(K2T31)_2$ (trans)	105.33
$Cu(K2T21)_2$	107.46
$Cu(Curcumin)_2$	110.15
K2T31	86.26
K2T21[b]	86.52
Curcumin[b]	86.83

[a] O-H BDE = TE_R + TE_H - TE_C
TE_R = total electronic energy of the radical derived from H-abstraction from the phenolic hydroxyl;
TEH = total electronic energy of H-atom (-0.500273 hartree);
TEC = total electronic energy of metal complex;
[b] taken from ref. 25

Table 3. λ_{max} (nm), hypochromism (%), red shift (nm) and calculated binding constant K_b (M^{-1}) for Cu-curcumin and Cu-K2T in 1:1 molar ratio.

Ligand	*λ_{max} (nm)*	*Hypochromism (%)*	*Red shift (nm)*	*Binding constant K_b (M^{-1})*
Curcumin	365	14.7	3	5.21×10^4
K2T21	428	18.2	2	1.08×10^4
K2T31	412	14.7	6	1.11×10^4
K2T24	410	7.4	3	1.45×10^3
K2T23	410	6.6	3	7.14×10^3

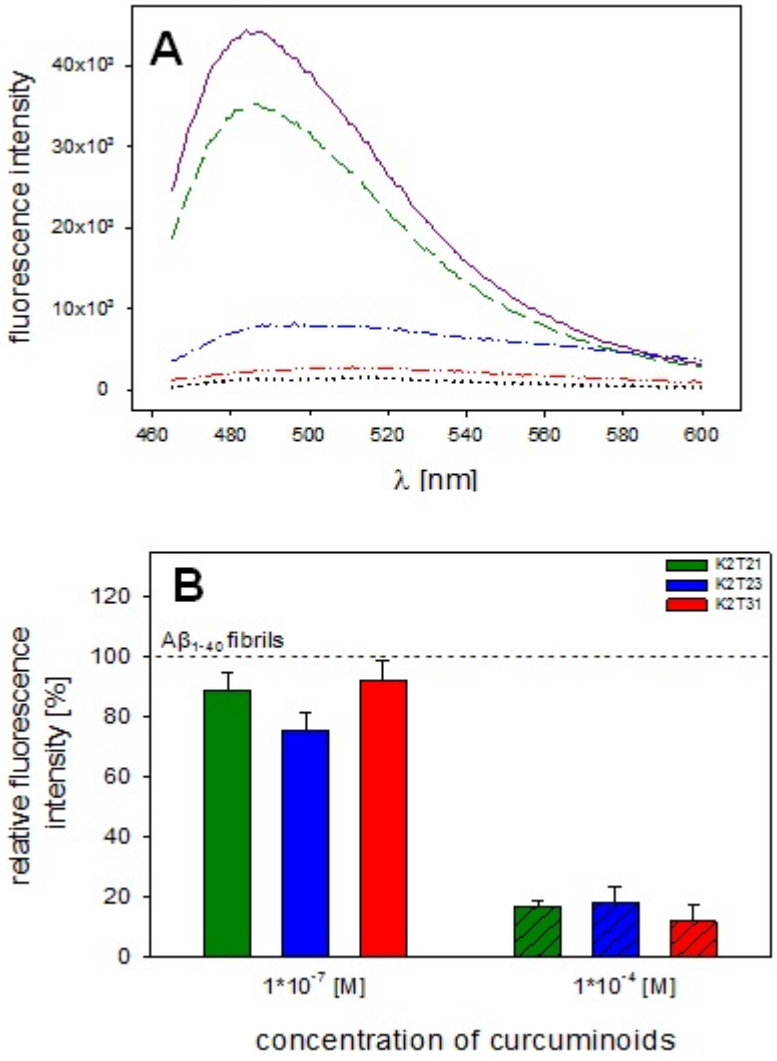

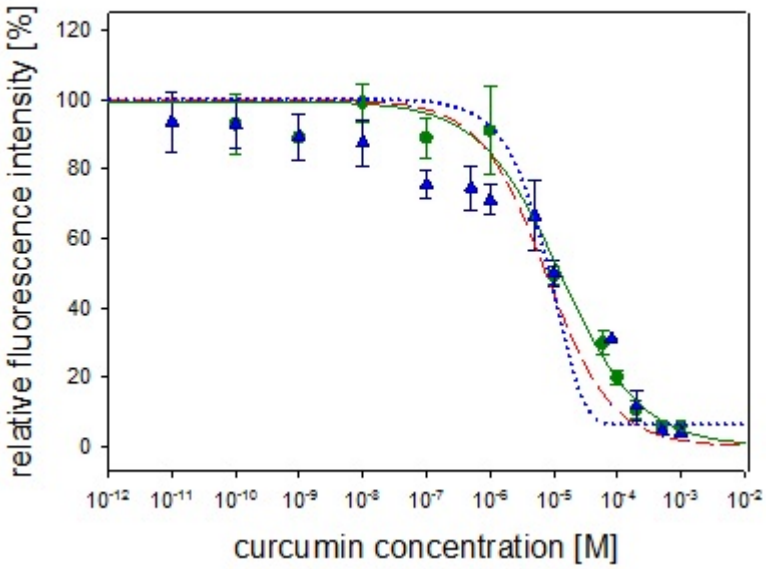

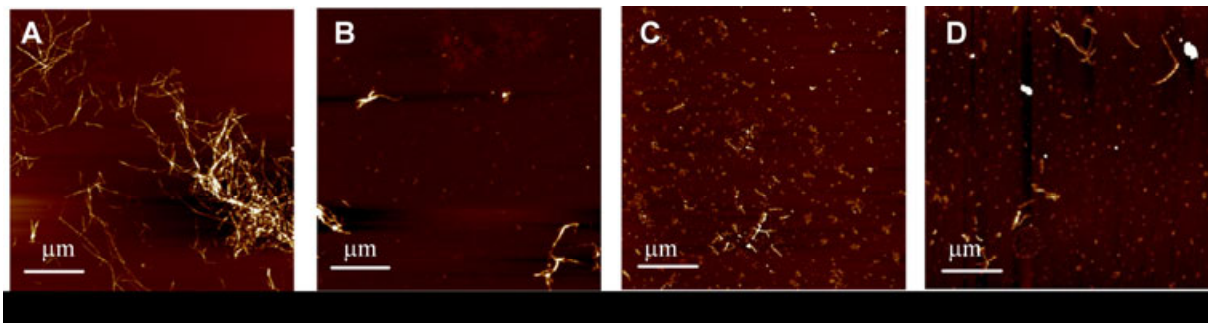

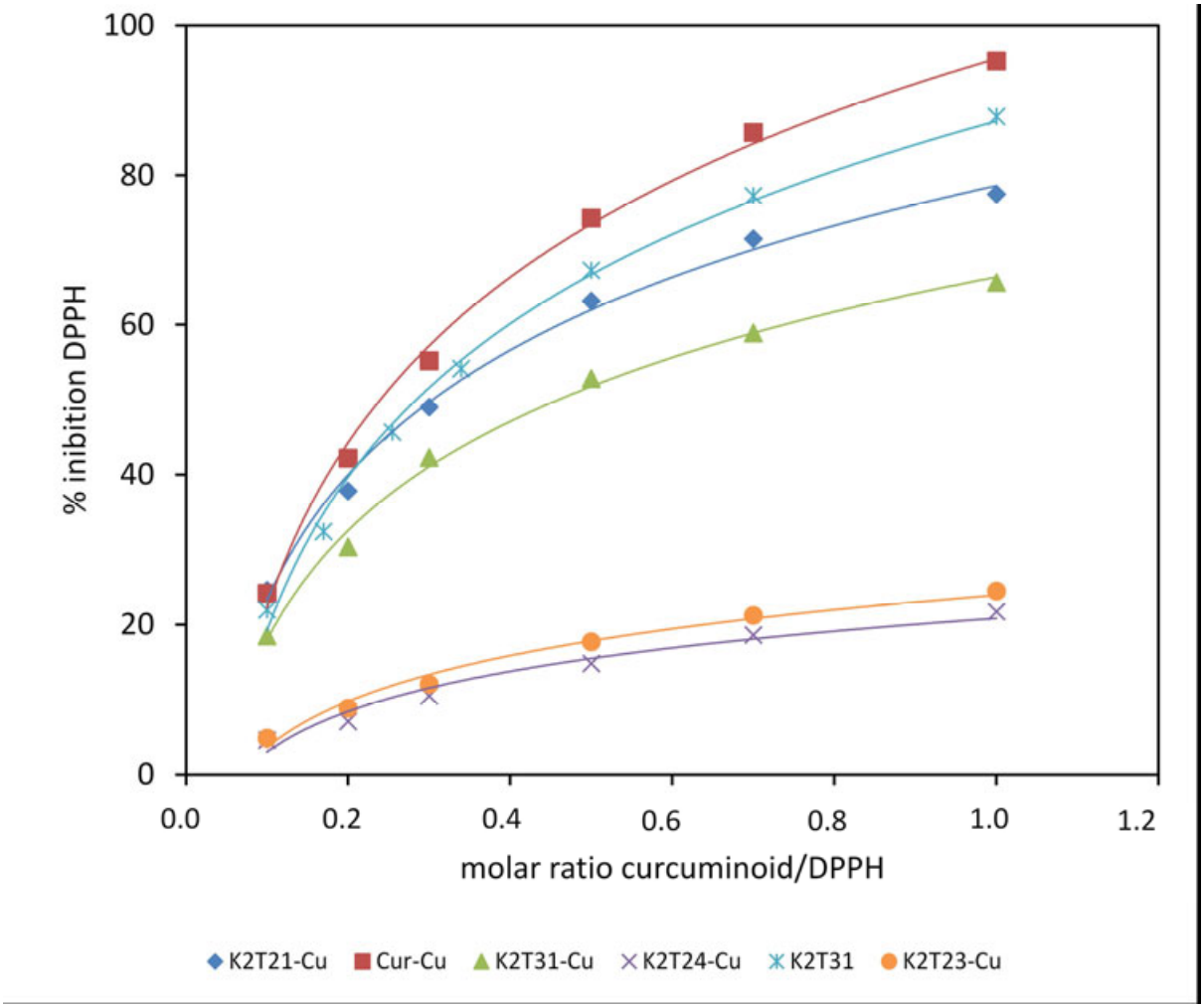

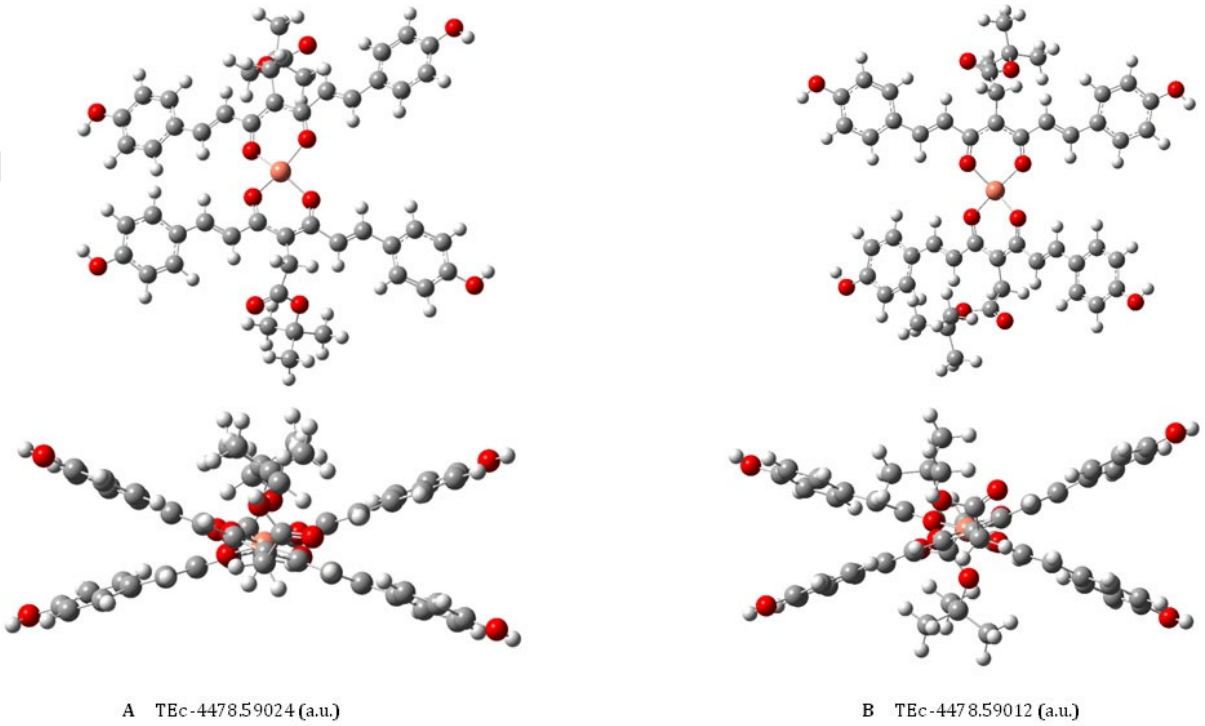

A TEc -4478.59024 (a.u.)

B TEc -4478.59012 (a.u.)

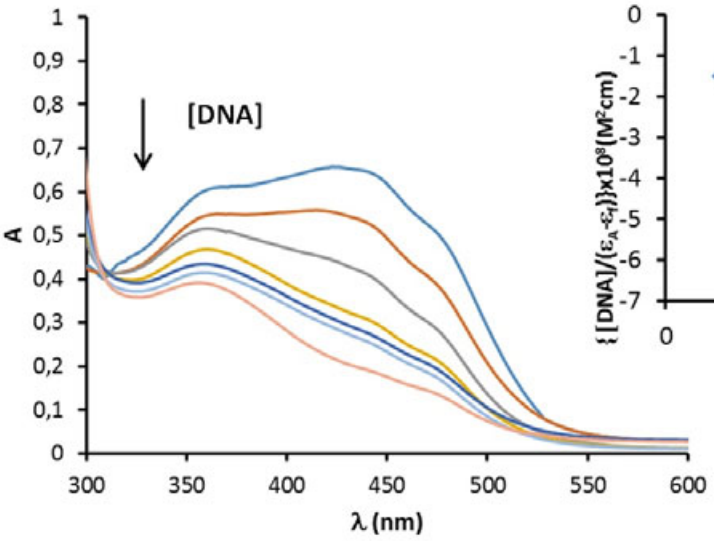

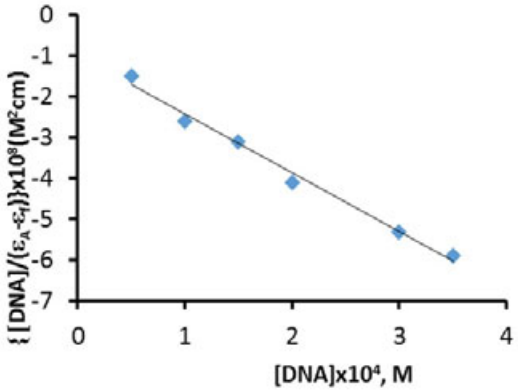

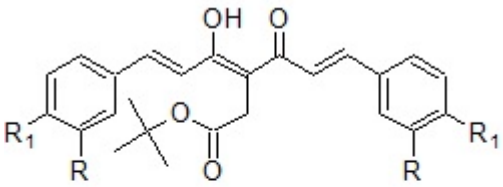

	R	R_1
K2T21 (1)	OCH_3,	OH
K2T23 (2)	OCH_3	H
K2T24 (3)	OCH_3	$OCOCH_3$
K2T31 (4)	H	OH